LA-UR- 95-3945

CONF-960238--6

Title: Comparison of Damage Identification Algorithms on Experimental Modal Data from a Bridge

Author(s): David V. Jauregui, LANL, ESA-EA
Charles R. Farrar, LANL, ESA-EA

Submitted to: 14th International Modal Analysis Conference
Dearborn, Michigan
February 12-15, 1996

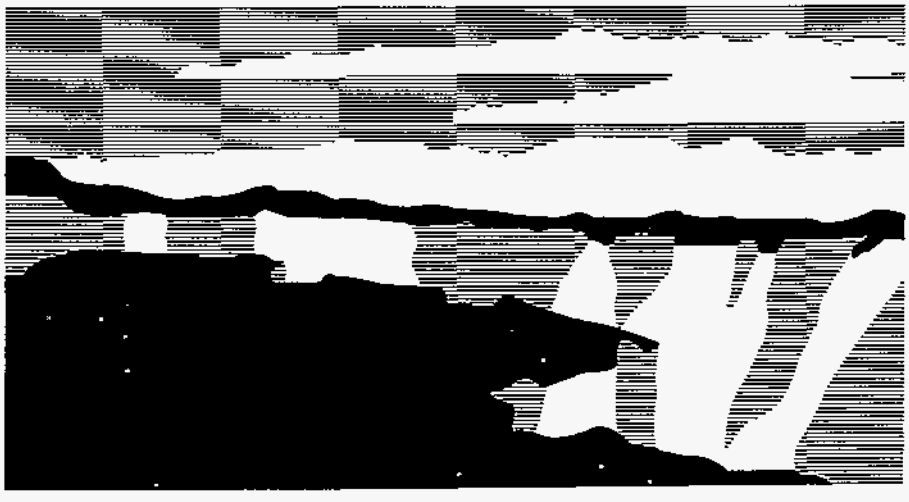

Los Alamos
NATIONAL LABORATORY

Form No. 836 R5
ST 2629 10/91

COMPARISON OF DAMAGE IDENTIFICATION ALGORITHMS ON EXPERIMENTAL MODAL DATA FROM A BRIDGE

David V. Jauregui and Charles R. Farrar

Engineering Analysis Group (ESA-EA)
MS P946
Los Alamos National Laboratory
Los Alamos, NM 87545

ABSTRACT. Over the past 25 years detecting damage in a structure from changes in dynamic parameters has received a considerable amount of attention from the aerospace, civil, and mechanical engineering communities. The general idea is that changes in the structure's physical properties (i.e., stiffness, mass, and/or damping) will, in turn, alter the dynamic characteristics (i.e., resonant frequencies, modal damping, and mode shapes) of the structure. Properties such as the flexibility matrix, stiffness matrix, and mode shape curvature, which are obtained from modal parameters, have shown promise for localizing structural damage. In this paper, several different techniques for damage assessment are demonstrated and compared using experimental modal data from an undamaged and damaged bridge.

1. INTRODUCTION.

Because the Interstate 40 (I-40) bridges over the Rio Grande in Albuquerque, New Mexico were to be razed during the summer of 1993, investigators from New Mexico State University (NMSU) were able to introduce simulated cracks into the structure in order to test various damage identification methods. To support this research effort, Los Alamos National Laboratory (LANL) performed experimental modal analyses [1, 2], and developed experimentally verified numerical models of the bridge [3].

In this paper five damage identification methods that have been reported in the technical literature were applied to the experimental modal data measured on the I-40 Bridge. Subsequently, the same methods were applied to numerically generated modal data obtained from the finite element models previously mentioned as discussed in an accompanying paper [4].

Length limitations of this paper preclude a detailed discussion of the experimental modal analyses. The pertinent data obtained from both the experimental studies, required by all of the damage identification algorithms, were resonant frequencies and mode shapes for the undamaged and damaged bridge. For a more detailed summary of the tests performed on the I-40 Bridge and the results that were obtained, the reader is referred to [1].

2. I-40 BRIDGE GEOMETRY AND DAMAGE SCENARIOS

The I-40 Bridge over the Rio Grande formerly consisted of twin spans (there are separate bridges for each traffic direction) made up of a concrete deck supported by two welded-steel plate girders and three steel stringers. Shear studs were not found when the concrete deck was removed. Loads from the stringers are transferred to the plate girders by floor beams located at 20-ft (6.1 m) intervals. Cross-bracing is provided between the floor beams. Figure 1 shows an elevation view of the portion of the bridge that was tested. The cross-section geometry of each bridge is shown in Fig. 2. It should be noted that the actual bridges have concrete crash barriers on either side of the concrete slab. Each bridge is made up of three identical sections. Except for the common pier located at the end of each section, the sections are independent. A section has three spans; the end spans are of equal length, approximately 131 ft (39.9 m), and the center span is approximately 163 ft (49.4 m) long. Five plate girders are connected with four bolted splices to form a continuous beam over the three spans. The portions of the plate girders over the piers have increased flange dimensions, compared with the midspan portions, to resist the higher bending stresses at these locations. Connections that allow for thermal expansion as well as connections that prevent longitudinal translation are located at the base of each plate girder, where the girder is supported by a concrete pier or abutment. These connections are labeled "exp" and "pinned" in Fig. 1.

The damage that was introduced was intended to simulate fatigue cracking that has been observed in plate-girder bridges. This cracking results from out-of-plane bending of the web at locations where the seats of the floor beams are

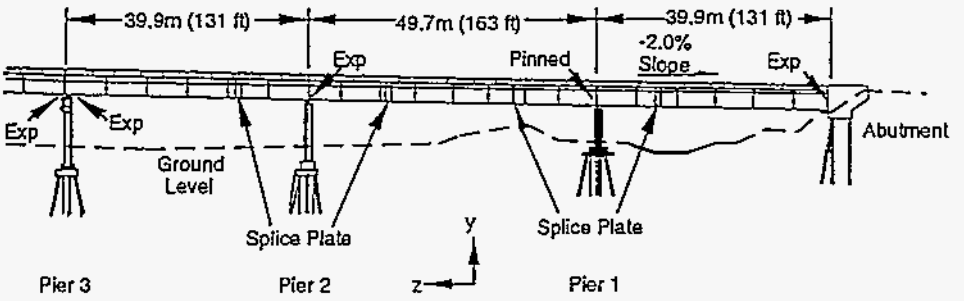

Fig. 1 Elevation view of the portion of I-40 bridge that was tested

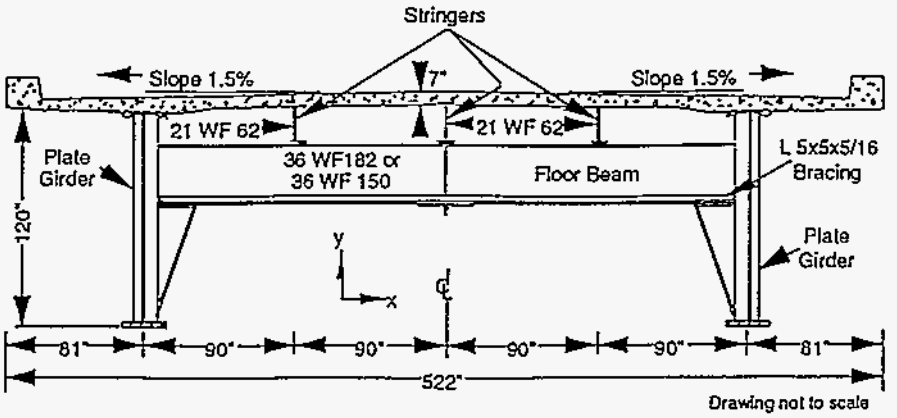

Fig. 2 Typical cross-section geometry of the I-40 bridge

welded to the web of the plate girder. Four levels of damage were introduced to the middle span of the north plate girder close to the seat supporting the floor beam at midspan. Damage was introduced by making torch cuts in the web and flange of the girder. The first level of damage, designated E-1, consisted of a two-foot-long (61.0 cm) cut through the web approximately 3/8-in-wide (0.95-cm-wide) centered at midheight of the web. Next, this cut was continued to the bottom of the web, E-2 . During this cut the web, on either side of the cut, bent out of plane approximately 1 in.(2.54 cm). The flange was then cut halfway in from either side directly below cut in the web, E-3. Finally, the bottom flange was cut completely through, E-4. The portions of the web and flange that were cut are shown in Fig. 3.

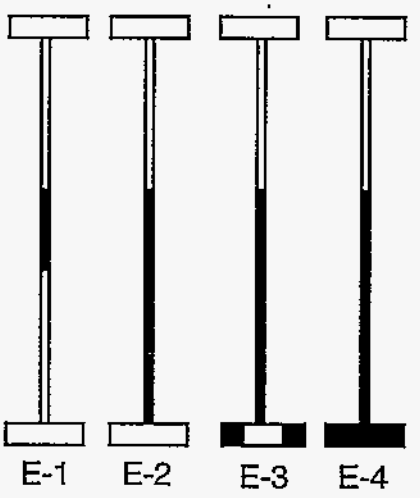

Fig. 3 Damage Scenarios

3. MODE SHAPE DATA

All the methods of damage identification discussed in Section 4 below examine changes in the mode shapes to locate the damage. Mode shapes were obtained from two sets of accelerometers. For the refined set of sensors (denoted SET1) shown in Fig. 4 eleven accelerometers were placed along the span where the damage was introduced. Experimental modal data were obtained from the amplitude and phase information of the cross-power spectra where sensor N-3 was used as a reference. This data reduction method simulates the mode shape identification method that would be used with ambient vibration data.

A course set of accelerometer data (denoted SET2) shown in Fig. 5 was also used. Modal data was determined from frequency response functions obtained during measured input, random, forced vibration tests. A rational-fraction polynomial, global, curve-fitting algorithm in a commercial modal analysis software package [5] was used to fit the analytical models to the measured FRF data and to extract resonant frequencies, mode shapes, and modal damping values. A random input at the location shown in Fig. 5 was used to excite the structure when data was acquired with either SET1 or SET2. Mode shape amplitude and phase information from SET1 and SET2 are listed in appendices in [1].

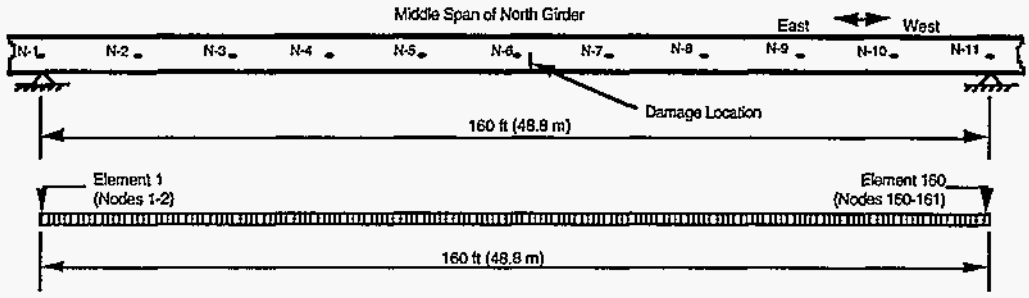

Fig. 4. Refined accelerometer locations.

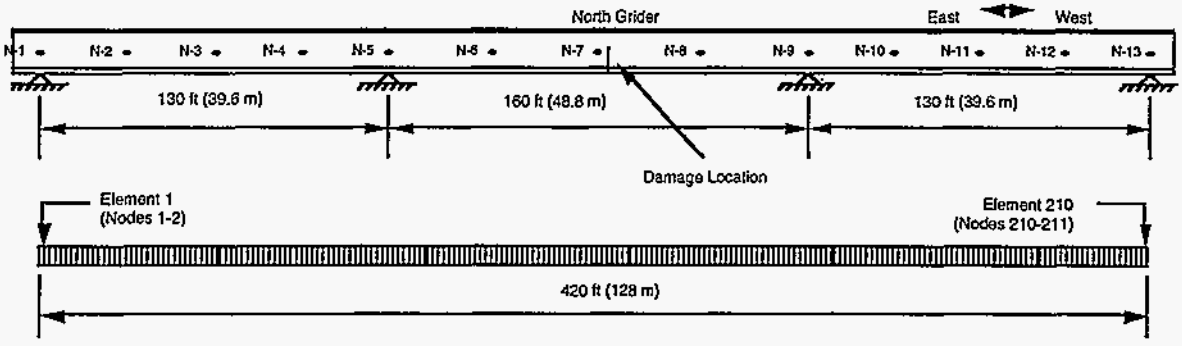

Fig. 5. Coarse accelerometer locations.

4. DESCRIPTION OF DAMAGE IDENTIFICATION METHODS

A very brief description of the damage identification methods that were used is given below. The reader is referred to the appropriate references for a more detailed discussion of these methods. A summary of their implementation for the study reported herein can be found in [6].

4.1 DAMAGE INDEX METHOD

The Damage Index Method was developed by Stubbs and Kim [7] to localize damage in structures given their characteristic mode shapes before and after damage. For a structure that can be represented as a beam, a damage index, β, based on changes in curvature of the ith mode at location j is defined as

$$\beta_{ji} = \frac{\left(\int_a^b [\psi_i^{*}{}''(x)]^2\,dx + \int_0^L [\psi_i^{*}{}''(x)]^2\,dx\right)}{\left(\int_a^b [\psi_i''(x)]^2\,dx + \int_0^L [\psi_i''(x)]^2\,dx\right)} \cdot \frac{\int_0^L [\psi_i''(x)]^2\,dx}{\int_0^L [\psi_i^{*}{}''(x)]^2\,dx}, \quad (1)$$

where $\psi_i''(x)$ and $\psi_i^{*}{}''(x)$ are the second derivatives of the ith mode shape corresponding to the undamaged and damaged structures, respectively. L is the length of the beam. a and b are the limits of a segment of the beam where damage is being evaluated. When more than one mode is used the damage index is the sum of damage indices from each mode. For mode shapes obtained from ambient data, the modes are normalized such that

$$\{\psi_n\}^T[m]\{\psi_n\} = 1, \quad (2)$$

where [m] is assumed to be the identity matrix [8].

To determine mode shape amplitudes at location between sensors, the mode shapes are fit with a cubic polynomial. As shown in Fig. 4 for the refined set of accelerometers, the middle span of the north girder is divided into 160 1-ft (0.305-m) segments. Modal amplitudes are interpolated for each of the 161 nodes forming these segments. Similarly, for the coarse set of accelerometers the entire length of the north girder (all three spans) is divided into 210 2-ft (0.610 m) segments with mode shape interpolation yielding amplitudes at 211 node locations as shown in Fig. 5.. Statistical methods are then used to examine changes in the damage index and associate these changes with possible damage locations. A normal distribution is fit to the damage indices, and values falling two or more standard deviations from the mean are assumed to be the most likely location of damage.

4.2 MODE SHAPE CURVATURE METHOD

Pandey, Biswas, and Samman [9] assume that structural damage only affects the stiffness matrix and not the mass matrix. Hence, for the undamaged and damaged condition the eigenvalue problems are given as

$$([K] - \lambda_i[M])\{\psi_i\} = \{0\}, \text{ and} \quad (3)$$

$$([K]^{*} - \lambda_i^{*}[M])\{\psi_i\}^{*} = \{0\}, \text{ respectively,} \quad (4)$$

where [K] = the stiffness matrix, λ_i = the ith eigenvalue, [M] = the mass matrix, ψ_i = the ith displacement eigenvector of

the undamaged structure, and the asterisks are quantities corresponding to the damaged structure. The pre- and post-damage eigenvectors extracted from this analysis are subsequently used for damage detection. Curvature of the mode shapes for the beam in undamaged and damaged condition can then be estimated numerically from the displacement mode shapes with a central difference approximation or other means of differentiation.

Given the before and after damage mode shapes, consider a beam cross section at location x subjected to a bending moment M(x). The instantaneous curvature at location x along the length of the beam, v" (x), is given by

$$v''(x) = M(x)/(EI), \tag{5}$$

where E = the modulus of elasticity, and
I = the moment of inertia of the section.

From this equation, it is evident that the curvature is directly proportional to the inverse of the flexural stiffness, EI. Thus, a reduction of stiffness associated with damage will, in turn, lead to an increase in curvature. Differences in the pre- and post-damage curvature mode shapes will, in theory, be largest in the cracked region. In [9] curvature is estimated from a central difference operator as

$$v''_{li} = \frac{\Psi_{(l+1)i} - 2\Psi_{(l)i} + \Psi_{(l-1)i}}{h^2}, \tag{6}$$

where h is the average distance between measurement points (actual or interpolated), v''_{li} is the curvature at point l corresponding to the ith mode, and ψ_{li} is the displacement at point l corresponding to the ith mode. Again, interpolation of the mode shape data as discussed in Section 4.2 was used to obtain mode shape amplitudes at locations between sensors. In this study, curvatures were estimated by differentiating the cubic polynomial that was fit to the mode shape amplitudes. For multiple modes the sum of the absolute differences in curvature are used to indicate damage.

4.3 CHANGE IN FLEXIBILITY METHOD

Pandey and Biswas [10] show that for the undamaged and damaged structure, the flexibility matrix, F, be approximated from the unit-mass-normalized modal data as follows

$$[F] \approx \sum_{i=1}^{n} \frac{1}{\omega_i^2} \{\phi_i\}\{\phi_i\}^T \text{ and} \tag{7}$$

$$[F]^* \approx \sum_{i=1}^{n} \frac{1}{\omega_i^{*2}} \{\phi_i\}^*\{\phi_i\}^{*T}, \tag{8}$$

where ω_i = the ith modal frequency, ϕ_i = the ith unit-mass-normalized mode, n = the number of measured modes, and the asterisks signify properties of the damaged structure. The approximation comes from the fact that fewer modes are typically identified than the total numbers of measurement points or degrees of freedom. From the pre- and post-damage flexibility matrices, a measure of the flexibility change caused by the damage can be obtained from the difference of the respective matrices as

$$[\Delta F] = [F] - [F]^*, \tag{9}$$

where [ΔF] represents the change in flexibility matrix. Now, for each column of this matrix let $\bar{\delta}_j$ be the absolute maximum value of the values in that column. Hence,

$$\bar{\delta}_j = \max\left|\delta_{ij}\right|, \quad i=1...n, \tag{10}$$

where δ_{ij} are elements of matrix [ΔF] and $\bar{\delta}_j$ is taken to be a measure of the flexibility change at each measurement location, j. The column of the flexibility matrix corresponding to the largest change is indicative of the degree of freedom where the damage is located. Interpolation to obtain intermediate mode shape amplitudes was again employed with this method.

4.4 CHANGE IN UNIFORM FLEXIBILITY CURVATURE METHOD

The coefficients of the ith column of the flexibility matrix represent the deflected shape assumed by the structure with a unit load applied at the ith degree of freedom. The sum of all columns of the flexibility matrix represent the deformed shape if a unit load is applied at each degree of freedom, and this shape is referred to as the uniform load flexibility. Zhang and Aktan [11] state that the change in curvature of the uniform load flexibility surface can be used to determine the location of damage. In terms of the curvature of the uniform load flexibility surface, F", the curvature change at location l is evaluated as follows

$$\Delta F''_l = \left|F''^*_l - F''_l\right|, \tag{11}$$

where ΔF" represents the absolute curvature change.

Again, the curvature of the uniform load flexibility shape at location l, F''_l, can be obtained with a central difference operator as

$$F''_l = \frac{f_{(l+1)} - 2f_{(l)} + f_{(l-1)}}{h^2} \tag{12}$$

where F are the displacements of the uniform load flexibility surface at location l+1, l, and l-1, respectively, and h is the average distance between measurement locations. Interpolation is employed to obtain data at locations between measurement points. However, in this study the curvature was obtained by differentiating a cubic polynomial that was fit to the uniform load flexibility shape.

4.5 CHANGE IN STIFFNESS METHOD

Investigation of the eigenvalue problem of a structure after the onset of damage has revealed information for detecting damage as discussed by Zimmerman and Kaouk [12]. The eigenvalue problem of a undamaged, undamped structure is stated as

$$(\lambda_i[M] + [K])\{\psi_i\} = \{0\}, \quad (13)$$

The eigenvalue problem of the damaged structure is formulated by first replacing the pre-damaged eigenvectors and eigenvalues with a set of post-damaged modal parameters and, second, subtracting the perturbations in the mass and stiffness matrices from the original matrices. Letting ΔM_d and ΔK_d represent the perturbations to the original mass and stiffness matrices, the eigenvalue equation expands to

$$\left[\lambda_i^*[M-\Delta M_d] + [K-\Delta K_d]\right]\{\psi_i\}^* = \{0\}, \quad (14)$$

Two forms of a damage vector D for the ith mode are then obtained by separating the terms containing the original matrices from those containing the perturbation matrices. Hence,

$$\{D_i\} = \left(\lambda_i^*[M]+[K]\right)\{\psi_i\}^* = \left(\lambda_i^*[\Delta M_d]+[\Delta K_d]\right)\{\psi_i\}^*. \quad (15)$$

To simplify the investigation, damage is usually considered to effect only the stiffness of a structure since substantial damage must occur to disrupt the mass. Therefore, the damage vector reduces to

$$\{D_i\} = [\Delta K_d]\{\psi_i\}^*. \quad (16)$$

The stiffness matrices, before and after damage, can be approximated from incomplete modal data by

$$[K] \approx \sum_{i=1}^{n} \omega_i^2 \phi_i \phi_i^T, \quad (17)$$

$$[K]^* \approx \sum_{i=1}^{n} \omega_i^{*2} \phi_i^* \phi_i^{*T}, \quad (18)$$

and subtracted to obtain the perturbation in stiffness matrix. Interpolation was again used to generate additional modal amplitudes. A scaling procedure discussed in [12] was used to avoid spurious readings at stiff locations where the signal-to-noise ratio is lower.

5. APPLICATION OF DAMAGE IDENTIFICATION METHODS TO EXPERIMENTAL DATA

In this section, the linear damage identification methods are exercised using experimental modal data from the I-40 Bridge. When applying the damage identification algorithms to experimental or analytical data, values of the mode shape amplitudes at location between sensors were determined by fitting either a cubic spline or a cubic polynomial to the data from the measurement locations as discussed in Section 4.2. Figures 6 through 10 show plots of the results from the different damage identification methods corresponding to the 160 intervals as determined from the refined set of accelerometers applied to damage scenario E-4. For this most severe case all methods located the damage.

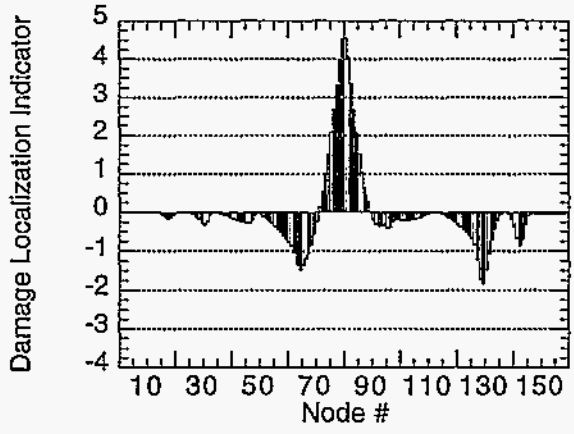

Fig. 6 Results of damage index method applied to modal data from damage scenario E-4.

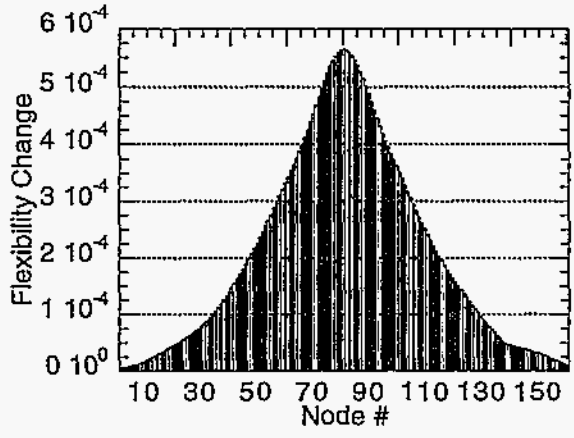

Fig. 7 Results of change in flexibility method applied to modal data from Damage scenario E-4

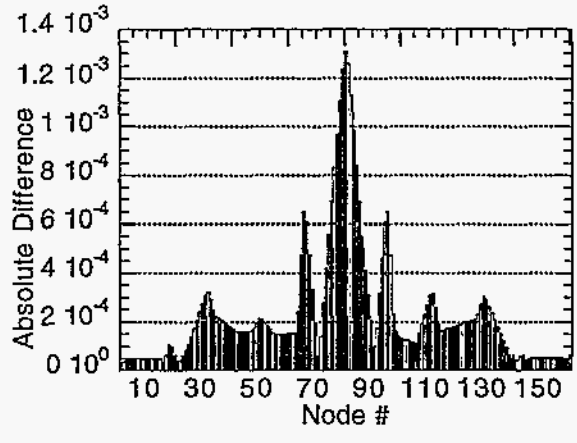

Fig. 8 Results of change in change in curvature method applied to modal data from Damage scenario E-4

Tables I and II summarize the results from applying the five damage detection algorithms to the experimental modal data. According to the tables, the Damage Index Method performed the best. The Mode Shape Curvature Method also

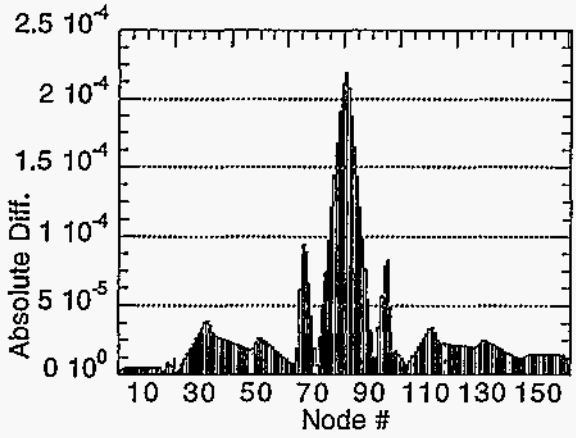

Fig. 9 Results of change in uniform flexibility curvature method applied to modal data from Damage scenario E-4

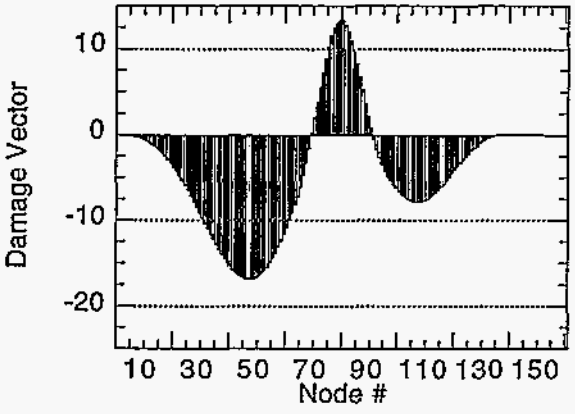

Fig. 10 Results of change in stiffness method applied to modal data from Damage scenario E-4

performed well, although not as well as the Damage Index Method. The Change in Flexibility Method appeared to have problems identifying damage for situations when damage was not severe. The Change in Uniform Flexibility Curvature Method performed satisfactorily using the experimental modal data from the refined set of accelerometers (SET1). The algorithms failed only for damage case E-1. Surprisingly, the Change in Stiffness Method improved when applied to the modal data from the coarse set of accelerometers. Significant improvements were also shown when only the first two modes were used instead of all six as shown in Table II. Using the refined measurements, only the final damage case (E-4) was detected with this method, whereas all damage cases were detected from the SET2 modal data. One possible explanation for this observation is that to calculate the stiffness matrix, unit-mass-normalized mode shapes are needed, and only SET2 are unit-mass normalized modes.

6. SUMMARY AND CONCLUSIONS

The application of five linear damage identification routines using experimental and numerical modal data gathered from the I-40 Bridge has been reported. In this case linear damage identification implies that linear dynamic models are used to model the structure both before and after damage has occurred. The nature of the damage applied to the I-40 bridge is such that the linear damage models are applicable to these damage scenarios. This study provides a direct comparison of various damage identification algorithms when applied to a standard problem. The authors are not

TABLE I

Summary of Damage Detection Results using Experimental Modal Data from Refined Set of Accelerometers (SET1)

Damage Case	E-1	E-2	E-3	E-4
Damage Index Method	•	•	•	•
Mode Shape Curvature Method	•••	••	•	•
Change in Flexibility Method	○	○	○	•
Change in Uniform Flexibility Curvature Method	○	•••	•	•
Change in Stiffness Method	○	○	○	•

• Damage located, •• Damage narrowed down to two locations, ••• Damage narrowed down to three locations, ○ Damage not located

TABLE II

Summary of Damage Detection Results using Experimental Modal Data from Refined Set of Accelerometers (SET2)

Damage Case	E-1	E-2	E-3	E-4
Damage Index Method	**	**	**	*
Mode Shape Curvature Method	**	*	**	*
Change in Flexibility Method	○	○	**	*
Change in Uniform Flexibility Curvature Method	○	○	○	*
Change in Stiffness Method	**	**	**	*

* Damage located, ** Damage located using only 2 modes; ○ Damage not located

aware of other such comparisons that have been reported in the technical literature.

Results of this study show that the damage index method performed the best. This method was the only one that detected and located damage at all four stages using either the refined or coarse set of accelerometers. This performance is considered noteworthy when one considers that the lowest level of damage, corresponding to only a 0.15 % reduction in the cross-section moment of inertia at the damage location, was located with the coarse set of accelerometers using only two measured modes.

Another observation from this study, which the authors feel is important, is that the damage index method is the only method tested that has a specific criteria for determining if damage has occurred at a particular location. The other methods only look for the largest change in a particular parameter and it is ambiguous at times to determine if these changes indicate damage at more than one location. This ambiguity is illustrated in Figs. 8 and 9 where, in a blind test, it would be difficult to tell if damage has occurred at one or three locations. This point is further studied with numerical models in the accompanying paper [4].

7. ACKNOWLEDGMENTS

Funding for this research was provided to New Mexico State University by the Federal Highway Administration. NMSU, in turn, contacted Los Alamos National Laboratory to perform the analyses reported herein.

8. REFERENCES

1. Farrar, C. R., et al., (1994) "Dynamic Characterization and Damage Detection in the I-40 Bridge over the Rio Grande," Los Alamos National Lab report LA-12767-MS.

2. Farrar, C. R. and K. M. Cone (1995) "Vibration Testing of the I-40 Bridge Before and After the Introduction of Damage," Proceedings 13th International Modal Analysis Conference, Nashville, TN.

3. Farrar, C. R., et al., (1995) "Finite Element Analysis of the I-40 Bridge over the Rio Grande," Los Alamos National Lab report LA-12979-MS.

4. Jauregui, D. V. and C. R. Farrar (1996) "Damage Identification Algorithms Applied to Numerical Modal Data from a Bridge," Proceedings 14th International Modal Analysis Conference, Dearborn, MI.

5. Structural Measurements Systems (1987), Modal 3.0, San Jose, CA.

6. Farrar, C. R. and D. V. Jauregui (1995) "Damage Detection Algorithms Applied to Experimental and Analytical Modal Data from the I-40 Bridge," Los Alamos National Lab report (in print).

7. Stubbs, N., J.-T. Kim, and C. R. Farrar (1995), *Field Verification of a Nondestructive Damage Localization and Severity Estimation Algorithm,* Proceedings 13th International Modal Analysis Conference, Nashville, TN.

8. Clough, R. W. and J. Penzien (1993) *Dynamics of Structures*, 2nd. Ed., McGraw Hill, New York.

9. Pandey, A. K., M. Biswas, and M. M. Samman (1991) "Damage Detection from Changes in Curvature Mode Shapes," *J. of Sound and Vibration*, 145(2), 321-332.

10. Pandey, A. K. and M. Biswas (1994) "Damage Detection from Changes in Flexibility," *J. of Sound and Vibration*, 169(1), 3-17.

11. Zhang, Z., and A. E. Aktan (1995) "The Damage Indices for the Constructed Facilities," *Proceedings of the 13th International Modal Analysis Conf.*, 2, 1520-1529.

12. Zimmerman, D. C. and M. Kaouk (1994) "Structural Damage Detection using a Minimum Rank Update Theory", *J.of Vibration and Acoustics*, 116, 222-231.